P H Y S I C A L R E V I E W L E T T E R S

Entanglement, Dephasing, and Phase Recovery via Cross-Correlation Measurements of Electrons

I. Neder, M. Heiblum, D. Mahalu, and V. Umansky

*Braun Center for Submicron Research, Department of Condensed Matter Physics, Weizmann Institute of Science,
Rehovot 76100, Israel*

Determination of the path taken by a quantum particle leads to a suppression of interference and to a classical behavior. We employ here a quantum "which path" detector to perform accurate path determination in a two-path Mach-Zehnder electron interferometer, leading to full suppression of the interference. Following the dephasing process we recover the interference by measuring the cross correlation between the interferometer and detector currents. Under our measurement conditions every interfering electron is dephased by approximately a single electron in the detector—leading to mutual entanglement of approximately single pairs of electrons.

Experiments involving electron interferometers coupled to a "path detector" are not new [1,2], however, they resulted only in partial dephasing of the interferometer. Here we take two steps forward: By constructing a highly sensitive detector, merely 1–3 detector electrons suffice to fully dephase the interferometer. Moreover, after the interference is quenched, we recover it by measuring the cross correlation of the dephased interferometer and the detector outputs. This is equivalent to "post selection" (or "coincidence") measurements in entangled photons systems [3–5]. There, when each of the entangled photons (*signal* and *idler*) was allowed to interfere with itself, interference was absent (each photon served as a detector of the other). The interference was fully recovered by coincidence measurements of events in the *signal* and in the *idler* sides. This, in effect, selects only some of the events (a post selection process). We followed a similar process in the present experiment.

We utilized an electronic Mach-Zehnder interferometer (MZI) [6,7], which we used before and demonstrated high visibility interference. Fabricated with a two-dimensional electron gas (see Fig. 1), the MZI operates in the integer quantum Hall effect regime (IQHE). An edge channel is split by a quantum point contact QPC1 to two paths that enclose a high magnetic flux and join again in point contact QPC2. Ohmic contacts serve as sources (*S*1, *S*2, *S*3) and drains (*D*1, *D*2). Changing the flux by $\Delta\Phi$ [by changing the area via biasing the modulation gate (MG)], alters the Aharonov-Bohm (*AB*) phase difference between the paths, $\varphi_{AB} = 2\pi\Delta\Phi/\Phi_0$ (Φ_0 the flux quantum) [8]. The phase dependent transmission coefficient from source *S*2 to drain *D*2 is

$$T_{\mathrm{MZI}} = |t_{\mathrm{QPC1}}t_{\mathrm{QPC2}} + e^{i\varphi_{AB}}r_{\mathrm{QPC1}}r_{\mathrm{QPC2}}|^2$$
$$= T_0 + T_\varphi\cos\varphi_{AB}, \qquad (1)$$

where *t* and *r* are the transmission and reflection amplitudes. The visibility $\nu = T_\varphi/T_0$ is found to be 30%–60% [6,8]. As we elaborate later, its value is limited most likely due to fluctuations in the enclosed flux caused by external

noise sources [9]. Note that a change in area of only some 200 nm^2 suffices to change the *AB* phase by 2π.

The detector was constructed as follows. Tuning the magnetic field to filling factor 2 in the IQHE, two edge channels, an outer and an inner, were injected at elevated electrochemical potentials by sources *S*2 and *S*3. Point contact QPC0 was tuned to fully transmit the outer channel and fully or partly reflect the inner one. Consequently, two channels impinged on QPC1: a fully occupied outer channel from *S*2 and a partitioned inner channel from both *S*2 and *S*3. In turn, we tuned $T_{\mathrm{QPC1}} = T_{\mathrm{QPC2}} = 0.5/0$ for the outer/inner channel. As a result, while the outer channel split and later interfered, the inner one flowed in close proximity to the upper path of the outer channel—serving as a "which path" detector.

Dephasing, or path detection, results from Coulomb interactions between electrons in the inner and outer channels. This interaction can be quantified experimentally before performing the actual dephasing experiment, by
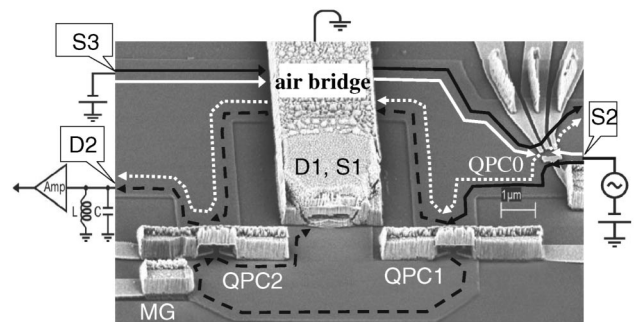

FIG. 1. Scanning electron microscope micrograph of the actual MZI and the detector. The inner contact (*D*1) and the two QPCs are connected with air bridges. The sample is defined by etching the GaAs-AlGaAs heterostructure that embeds a high mobility 2D electron gas. Magnetic field of ~3 T leads to filling factor 2 in the bulk (electron temperature ~15 mK). The signal at *D*2 is filtered by a cold LC resonant circuit at a center frequency ~1 MHz and bandwidth ~100 kHz. It is amplified *in situ* by a low noise preamplifier cooled to 4.2 K.

036803-1

fully reflecting the inner channel with point contact QPC0, so that it arrives noiseless from S3, hence functioning as a biased "gate" to the MZI upper path, with $V_{det} = V_{S3} - V_{S2}$. Changing V_{det} changed the enclosed MZI area, hence the AB phase, with $\sim 2\pi$ for $\Delta V_{det} = 20$ μV, but not the visibility of the MZI (see Fig. 2 in Ref. [10]).

Splitting now the detector beam into two paths (with point contact QPC0), partitions the detector channel while providing a reference path for an "in principle" measurement of the detector's phase. This phase is sensitive to a presence of an electron in the upper path of the MZI; hence, detection process, which leads to phase scrambling by the detector shot noise [11], and dephasing. Formally, after the interaction, the interferometer and detector wave function is an entangled state:

$$|\Psi\rangle = |\psi_l\rangle \otimes |\chi_l\rangle + e^{i\varphi_{AB}}|\psi_u\rangle \otimes |\chi_u\rangle, \qquad (2)$$

where $|\psi_{l,u}\rangle$ the interferometer's partial wave functions with an electron in the lower or upper paths, $|\chi_{l,u}\rangle$ the corresponding detector wave functions, and φ_{AB} the AB phase. If the outgoing wave function of an electron in drain D2 is $|D_2\rangle$, then the probability to find the interfering electron in D2 is $P = |\langle D_2|\Psi\rangle|^2$, namely,

$$P = |\langle\psi_l|D_2\rangle|^2 + |\langle\psi_u|D_2\rangle|^2$$
$$+ 2\mathrm{Re}[e^{i\varphi_{AB}}\langle\psi_l|D_2\rangle\langle D_2|\psi_u\rangle\langle\chi_l|\chi_u\rangle]. \qquad (3)$$

The overlap of detector states that multiply the interference term determines the visibility. For an absolute path determination and vanishing interference, the two detector states must be orthogonal.

The two detector's states $|\chi_{l,u}\rangle$ are generally complicated many-electron states [8]; however, here we consider a simple model with n-independent electrons in the detector channel interacting with an electron in the interferometer. Each of the detecting electron states can be expressed as follows: $|\chi_l\rangle_{1P} = t_d|t_d\rangle + r_d|r_d\rangle$ and $|\chi_u\rangle_{1P} = t_d|t_d\rangle + e^{i\gamma}r_d|r_d\rangle$, where $t_d|t_d\rangle$ and $r_d|r_d\rangle$ are the amplitudes of the transmitted and reflected electron wave functions (by point contact QPC0), with $T_{QPC0} = t_d^2$, $R_{QPC0} = r_d^2 = 1 - T_{QPC0}$, and γ the induced phase in the detector by an electron in the upper path of the interferometer. The visibility is [1,2,12]

$$|\langle\chi_l|\chi_u\rangle_{1P}|^n = \left(1 - 4t_d^2r_d^2\sin^2\frac{\gamma}{2}\right)^{n/2}, \qquad (4)$$

with $n \sim \frac{I_{det}\tau_d}{e} = \frac{eV_{det}\tau_d}{h}$ ($\frac{e^2}{h}$ the channel conductance), τ_d the dwell time of an electron in the upper path of the MZI, $\tau_d = \frac{L}{v_g}$. For $V_{det} = 20$ μV, MZI path length $L \approx 10$ μm and estimated drift velocity $v_g \sim (2\text{--}5)10^6$ cm/sec, only some 1–2.5 electrons are required for an accurate path detection and phase shift $\sim 2\pi$. Note that here interactions are strong, in contrast with previous experiments [1,2], where $\gamma \ll \pi$ and dephasing resulted from many "weakly detecting electrons".

The effect of partitioning the inner channel, $T_{QPC0} \sim 0.5$, on the visibility of the MZI is shown in Fig. 2. With no effective detection the visibility is $\sim 30\%$ [Fig. 2(a)], but at $V_{det} = 24$ μV the visibility drops to merely $\sim 1.5\%$ [Fig. 2(b)], vanishing altogether as V_{det} increases further [Fig. 2(c)]. Moreover, the dependence of the visibility on
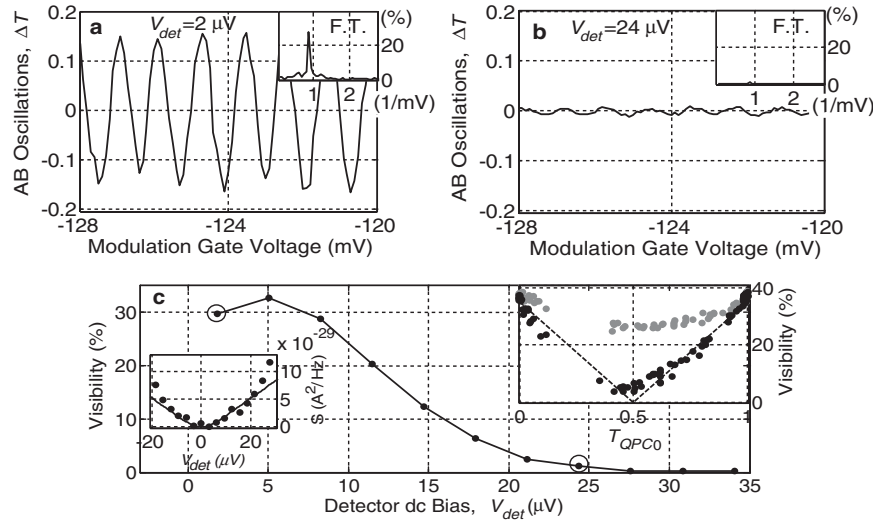

FIG. 2. Path determination leading to dephasing. (a) The transmission of the interferometer T_{MZI} oscillates as function of the modulation gate voltage with visibility $\nu \sim 35\%$ at $V_{S2} = 4.5$ μV (at $V_{S2} = 0$, $\nu \sim 45\%$, not shown). The Fourier transform has a peak at ~ 0.8 oscillation per 1 mV (inset). (b) At $V_{det} = 24$ μV the oscillations drop by more then an order of magnitude. The phase shift between Figs. 2(a) and 2(b) is meaningless, as the two graphs where measured at different times; hence slightly different magnetic fields. (c) The evolution of the visibility as function of V_{det} (the small increase in the visibility near $V_{det} = 5$ μV is due to resonances in point contact QPC0 at small V_{det}). Upper inset: The dependence of the visibility on T_{QPC0} for $V_{det} = 6$ μV (gray dots) and for 15 μV (black dots). The dotted line is the prediction of Eq. (4) with $\gamma = \pi$ and $n = 1$. Lower inset: Measured noise of the detector agrees with shot noise of independent electrons at $T = 15$ mK.

the partitioning determined by T_{QPC0} [Fig. 2(c), upper inset] changes from parabolic to V shape as V_{det} increases to 15 μV (minimum always at $T_{QPC0} = 0.5$). It is interesting to note that for $n = 1$ and $\gamma \sim \pi$, Eq. (4) indeed leads to a V-shape visibility $\nu \propto |1-2T_{QPC0}|$, in contrast to the measured second moment of the noise in the detector channel [lower inset in Fig. 2(c), $T_{QPC0} = 0.5$], which obeys $S_{det} = 2eV_{det}(e^2/h)T_{QPC0}(1-T_{QPC0})$ (with finite temperature corrections [13]). This is a manifestation of the effect of higher moments of the shot noise in the detector channel on the dephasing process.

Can the lost interference be recovered? Recall that dephasing the MZI results from averaging over the detector states, namely, over the presence of an electron (probability R_{QPC0}) or its absence (probability T_{QPC0}). If we were to select among the interfering electrons only those passing simultaneously with a detector electron, they would all acquire the same phase $\varphi_{AB} + \gamma$. We show first theoretically that such a post selection process is achieved via measuring the cross correlation between current fluctuations of the detector and of the MZI—provided that indeed one electron in the detector is coupled to an electron in the MZI.

For a fully dephased MZI, with $n = 1, \gamma = \pi, T_0 = 0.5$, The cross correlation (CC) between the total currents in the MZI and the detector is proportional to $\langle \Delta n_{MZI} \Delta n_{det} \rangle = \langle n_{MZI} n_{det} \rangle - \langle n_{MZI} \rangle \langle n_{det} \rangle$, with the fluctuating term given by: $\langle n_{MZI} n_{det} \rangle = \sum_{n_{MZI}, n_{det}=0,1} P(n_{MZI}|n_{det})P(n_{det})n_{MZI}n_{det}$, and $P(n_{MZI}|n_{det})$ the conditional probability that n_{MZI} (0 or 1) electrons exiting the MZI toward $D2$ provided that n_{det} (0 or 1) electrons exiting the detector channel toward $D2$. Here, the only nonvanishing term is $n_{MZI} = n_{det} = 1$, with $P(n_{det} = 1) = R_{QPC0} = 0.5$ and $P(n_{MZI} = 1|n_{det} = 1) = T_0 + T_\varphi \cos(\varphi_{AB} + \gamma)$. Hence for an inital visibility $\nu = T_\varphi/T_0$, the spectral density of the CC term is $S_{CC} = A\nu \cos(\varphi_{AB} + \gamma)$, with A prefactor. In other words, the CC term oscillates with the basic AB periodicity, even though the MZI is fully dephased.

The prefactor A can be roughly estimated in our "$n_{det} = 1$" model. We assume that the shot noise in the detector behaves as a switching noise, in the sense that the potential in the detector fluctuates randomly every time interval $\frac{e}{I_{det}} = \frac{h}{eV_{det}}$ between two possible values: V_{det} when an electron is present with probability R_{QPC0}, and 0 when it is absent with probability T_{QPC0}. Consequently, the current at the output of the MZI fluctuates between $V_{MZI} = V_{S2}T_0[1 + \nu\cos(\varphi_{AB} + \gamma)]$ and $V_{MZI} = V_{S2}T_0[1 + \nu\cos(\varphi_{AB})]$, respectively. This two-state model leads to

$$S_{CC} = 2\langle \Delta i_{MZI}\Delta i_{det} \rangle_{FT,f\to 0}$$
$$= 8eI_{S2}T_0\nu R_{QPC0}T_{QPC0}\sin(\gamma/2)\cos(\varphi_{AB} + \gamma/2).$$
(5)

At low detector bias the CC term [derived as a limit of Eq. (5)] has a simpler form: $S_{CC} = 2\langle \frac{di_{MZI}}{di_{det}}\Delta i_{det}\Delta i_{det} \rangle = 2\frac{di_{MZI}}{di_{det}}\langle \Delta i_{det}^2 \rangle$. The detector shot noise $\langle \Delta i_{det}^2 \rangle$ depends linearly on V_{det} [Fig. 2(c), lower inset] and $\frac{di_{MZ}}{di_{det}}$ is proportional to the *transconductance* through the measured phase dependence, $\frac{di_{MZI}}{di_{det}} = \frac{dV_{MZI}}{dV_{det}} = \frac{dV_{MZI}}{d\varphi}\frac{d\varphi}{dV_{det}} = V_{S2}T_0\nu\sin\varphi_{AB}\frac{2\pi}{20~\mu V}$. Hence, we expect the CC term to rise linearly with V_{det}, saturating at $\sim 1 \times 10^{-29}$ A^2/Hz at $V_{det} = 5~\mu$V for $T_0 = R_{QPC0} = T_{QPC0} = 0.5$.

In our system we have only a single drain ($D2$) for both MZI and detector. However, measuring the total current fluctuations in $D2$,

$$\langle (\Delta n_{D2})^2 \rangle = \langle (n_{MZI} + n_{det})^2 \rangle - (\langle n_{MZI} \rangle + \langle n_{det} \rangle)^2$$
$$= \langle (\Delta n_{MZI})^2 \rangle + \langle (\Delta n_{det})^2 \rangle + 2\langle \Delta n_{MZI}\Delta n_{det} \rangle,$$
(6)

provides the sought after CC term. As shown above, in a fully dephased MZI only the CC term is phase dependent. We performed noise measurements in $D2$ and analyze them below.
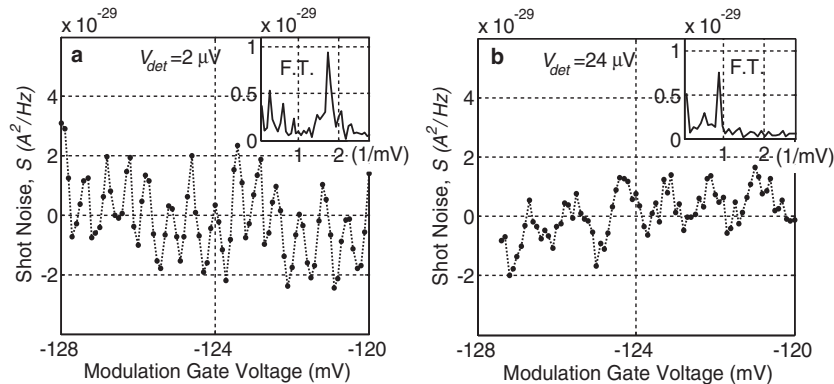

FIG. 3. Oscillatory component of the total noise. The total noise measured at $D2$ (at ~ 1 MHz, ~ 30 kHz bandwidth) as a function of V_{S3} with $V_{S2} = 4.5~\mu$V. It contains the contributions of the MZI, the detector, and their cross correlation. (a) For $V_{det} \sim 2~\mu$V, there is no dephasing. The noise is mostly that of the MZI (plotted around the average), having only a second AB harmonic. (b) For $V_{det} = 24~\mu$V, the AB oscillations of the conductance nearly vanish [Fig. 2(b)], however, the shot noise oscillates at the basic AB periodicity (plotted around the average).
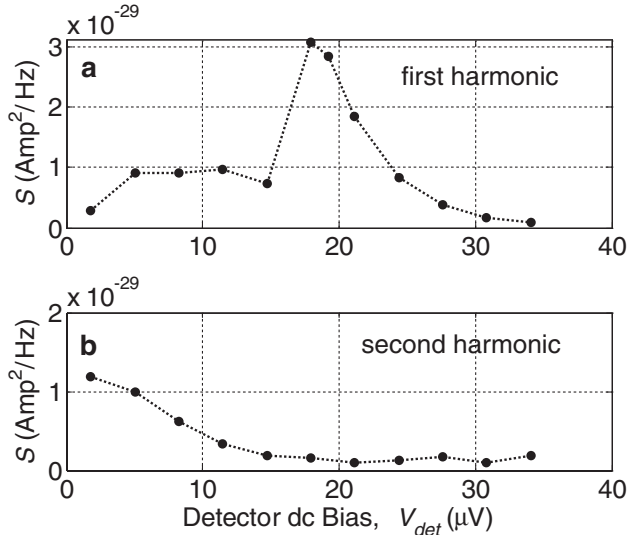
FIG. 4. Evolution of the *AB* harmonics in the total noise as a function of the detector voltage V_{det}. (a) The strength of the first *AB* harmonic. (b) The strength of the second *AB* harmonic. The following rapid increase at $V_{\text{det}} \sim 18 \ \mu\text{V}$ and the subsequent decrease are still not understood (see text).

We start with an unbiased detector, $V_{\text{det}} \sim 0$ ($\Delta n_{\text{det}} = 0$), with the shot noise in *D*2 only that of the interferometer: $S_{D2} = S_{\text{MZI}} = 2eI_{\text{imp}}T_{\text{MZI}}(1 - T_{\text{MZI}})$, with $I_{\text{imp}} = \frac{e^2}{h}V_{S2}$. In a symmetric interferometer $T_0 = 0.5$, $T_\varphi = 0.5\nu$ and $S_{D2} = 0.5eI_{\text{imp}}(1 - \nu^2\cos^2\varphi_{AB})$: shot noise oscillating only at the second *AB* harmonic. Slightly biasing the MZI with $V_{S2}(\text{DC}) = 4.5 \ \mu\text{V}$ in order to produce shot noise and retain the interference, led indeed to an oscillating shot noise as function of φ_{AB} [see short segment in Fig. 3(a), with a Fourier transform of some 13 *AB* periods in the inset]. Compared with the current oscillations in Fig. 2(a), the noise oscillated at exactly half the *AB* period. Note, however, that the amplitude of the oscillations in the noise was some 5 times higher than expected (for $\nu \sim 45\%$ at $V_{S2} = 0$). We account this large noise to an external (and unavoidable) noise, that led to fluctuations in the *AB* phase leading to $\Delta T_{\text{MZI}} \propto \Delta(T_\varphi \cos\varphi_{AB})$. Since the spectral density is proportional to $(\Delta T_{\text{MZI}})^2$, it oscillated, again, with the second *AB* harmonic; added to the shot-noise signal. The noise measurement explains the nonideal visibility, being a result of "phase averaging" due to external low frequency noise.

The evolution of the noise in *D*2 with increasing V_{det} was then measured. A short segment of such data is shown in Fig. 3(b) for an almost fully dephased interferometer ($V_{S2} = 4.5 \ \mu\text{V}$, $V_{\text{det}} = 24 \ \mu\text{V}$), with the total noise in *D*2 oscillating now only at the basic *AB* frequency. A summary of the evolution of the two *AB* harmonics in the noise as function of V_{det} is given in Fig. 4. As V_{det} increased the

second *AB* harmonic decreased and vanished altogether— a consequence of the quenched phase dependent transmission of the MZI. The first *AB* harmonic, though, appeared fast, saturated at around $1 \times 10^{-29} \ \text{A}^2/\text{Hz}$, and then grew abruptly with V_{det}. After reaching a new peak near $3 \times 10^{-29} \ \text{A}^2/\text{Hz}$ it fell and vanished near $V_{\text{det}} \cong 34 \ \mu\text{V}$. The strength of the CC, first *AB* harmonic, term agrees roughly with a simple estimate provided above, even though the exact dynamic of the electrons in the edge channels was not considered. The reasons for the deviations from our estimate, manifested in the sudden increase in the CC term near $V_{\text{det}} \sim 15$–$18 \ \mu\text{V}$ followed by the subsequent fall near $V_{\text{det}} > 25 \ \mu\text{V}$, are not clear. While the increase may be related to an onset of a second electron occupying the detector channel, the decrease at high V_{det} may result from a many electron picture (not the assumed $n = 1$), or due to new degrees of freedom in the detector, also unaccounted for in our model.

The strong interactions between adjacent edge channels allowed us to entangle approximately single pairs of electrons [14,15], one electron serving as a detector of the other's path. After the detected electron ceased to interfere, measuring the cross correlation between incidence events of the two electrons (actually, between current fluctuations in the two edge channels), the interference was recovered. A simple, one electron, theory nicely reproduced the data.

[1] E. Buks *et al.*, Nature (London) **391**, 871 (1998).
[2] D. Sprinzak *et al.*, Phys. Rev. Lett. **84**, 5820 (2000).
[3] A. Einstein, B. Podolsky, and N. Rosen, Phys. Rev. **47**, 777 (1935).
[4] D. V. Strekalov *et al.*, Phys. Rev. Lett. **74**, 3600 (1995).
[5] P. H. S. Ribeiro *et al.*, Phys. Rev. A **49**, 4176 (1994).
[6] Y. Ji *et al.*, Nature (London) **422**, 415 (2003).
[7] I. Neder *et al.*, Phys. Rev. Lett. **96**, 016804 (2006).
[8] Y. Aharonov and D. Bohm, Phys. Rev. **115**, 485 (1959).
[9] F. Marquardt, Europhys. Lett. **72**, 788 (2005).
[10] I. Neder *et al.*, cond-mat/0610634.
[11] A. Stern, Y. Aharonov, and J. Imry, Phys. Rev. A **41**, 3436 (1990).
[12] D. V. Averin and E. Sukhorukov, Phys. Rev. Lett. **95**, 126803 (2005).
[13] G. B. Lesovik, JETP Lett. **49**, 592 (1989).
[14] C. W. J. Beenakker, cond-mat/0508488.
[15] P. Samuelson, E. V. Sukhorukov, and M. Buttiker, Phys. Rev. Lett. **92**, 026805 (2004).